

MICHIGAN STATE UNIVERSITY

CYCLOTRON LABORATORY

MEAN FIELD DEFLECTION IN
PERIPHERAL HEAVY-ION COLLISIONS

W.K. WILSON, D. CEBRA, S. HOWDEN, J. KARN,
D. KROFCHECK, R. LACEY, T. LI, A. NADASEN,
T. REPOSEUR, A. VANDER MOLEN, C.A. OGILVIE,
G.D. WESTFALL, and J.S. WINFIELD



NOVEMBER 1990

MSUCL-750

MEAN FIELD DEFLECTION IN PERIPHERAL HEAVY-ION COLLISIONS

W.K. Wilson, D Cebra*, S. Howden, J. Kern, D. Krofcheck†,
R. Lacey, T. Li, A. Nadasen†, T. Reposeur, A. Vender Molen,

C.A. Ogilvie§, G.D. Westfall, and J.S. Winfield
*National Superconducting Cyclotron Laboratory and
Department of Physics and Astronomy
Michigan State University, East Lansing, MI 48824-1321, USA*

We have measured the transverse momentum of protons as a function of rapidity in 50 MeV/nucleon C induced peripheral collisions with C and Au targets. The reaction plane for each event was determined from the azimuthal angle of lightly damped coincident projectile fragments. Protons produced in the hot mid-rapidity region were found to be deflected towards the opposite side of the reaction plane with respect to the beam axis than the projectile fragments. This result is interpreted as projectile fragment scattering to positive angles due to the repulsive Coulomb interaction while participant protons are simultaneously deflected to negative angles by the attractive component of the nuclear mean field.

PACS 25.70Np

I. INTRODUCTION

At intermediate beam energies the transverse momentum flow changes direction due to a shift from attractive mean field dominated interactions at a few tens of MeV/nucleon to repulsive nucleon-nucleon scattering at a few hundreds of MeV/nucleon. The beam energy at which this change occurs has been shown to provide insight into the nuclear equation of state and the in-medium nucleon-nucleon cross section.^{1,2} Several recent experiments have attempted to extract this quantity for near-central events from data taken with large solid angle detector systems.^{2,3,4,5,6,7} Since theoretical calculations⁸ and experimental observations⁷ have suggested that collective flow in this beam energy range may change with impact parameter, we have performed a study of the transverse momentum of protons emitted in peripheral events.

In order to determine the reaction plane for low multiplicity peripheral events, we have used projectile-like fragments, which are expected to lie in the reaction plane. Analysis of two previous sets of polarization data^{9,10} suggested that there may be a complex interplay between attractive and repulsive scattering. Observation of the polarization of gamma rays produced by the heavy residue in 20 and 30 MeV/nucleon N induced reactions on a Sm target has shown⁹ that participant light particles are attractively deflected by the nuclear mean field. However, a study of the polarization of deflected projectile fragments produced in 40 MeV/nucleon N+Au reactions has been interpreted as repulsive scattering.¹⁰ Our observations reported here of 50 MeV/nucleon C on C and Au targets indicate that, once sequential decay products from the projectile fragment are eliminated from the analysis, participant protons show a directed transverse momentum opposite to that shown by the projectile frag-

ment, which provides a link between the conclusions of the two polarization experiments cited above.

II. EXPERIMENTAL DESCRIPTION AND ANALYSIS TECHNIQUES

A beam of ^{12}C was accelerated to 50 MeV/nucleon by the K500 Cyclotron at the National Superconducting Cyclotron Lab and focused on ^{12}C and ^{197}Au targets located inside the Michigan State University 4π Array.¹¹ The 170 phoswich telescopes of the Main Ball were used to detect protons of energies ≥ 18 MeV at polar angles from $\approx 18^\circ$ to $\approx 162^\circ$ with respect to the beam axis. Projectile fragments with velocities in excess of $\approx 70\%$ of the beam velocity were observed using a 45 element phoswich telescope Forward Array covering polar angles from 5.5° to 18° . Mass resolution of hydrogen isotopes in the Main Ball allowed separation of protons from other light particles while projectile fragments ($3 \leq Z \leq 6$) were identified by their charge in the Forward Array.

Velocity spectra for fragments detected in coincidence with protons are shown in Fig. 1 using $A=2Z$ to approximate the fragment masses. The spectra have been divided into three polar angle bins and normalized by the solid angles of the detectors. Both the C+C and the C+Au reactions produce fragment spectra with pronounced peaks close to the beam velocity.

Using the projectile fragment to determine the reaction plane, a coordinate system for each event was chosen such that the z axis lay along the beam axis and the positive x axis had the same azimuthal angle as the fragment. The momentum distribution of mid-rapidity protons ($y = \frac{1}{2}y_{\text{beam}}$) detected in the Main Ball is shown in Fig. 2 projected onto the P^x axis. In order to avoid discontinuities in the momentum dis-

tribution due to the granularity of the detector array, the polar and azimuthal angles assigned to the protons were smeared over the angular acceptance of the detectors. The usual procedure for measuring the directed transverse momentum in the reaction plane calls for plotting the average of this distribution, $\langle P^x \rangle$, as a function of rapidity.¹² The average, however, is affected by the detector low energy threshold which carves out a sphere in momentum space centered the origin and creates the dip observed in the center of the P^x distribution shown in Fig. 2. As a result, the average of the distribution will overestimate the magnitude of the offset from the origin, depending on the relationship between the distribution's width and the energy threshold of the detectors. In Refs. 2 and 3 this effect was minimized by calculating $\langle \frac{P^x}{|P_T|} \rangle$ which is significantly less sensitive to this threshold effect than $\langle P^x \rangle$. The overestimation of the offset can be eliminated entirely, however, if the center of the P^x distribution, P_0^x , is extracted by fitting a Gaussian to the regions in momentum space unaffected by the energy thresholds. This is the approach we have used in the present work.

In order to verify that the correlations observed in the data are not merely artifacts of our detector acceptance, we generated uncorrelated events from projectile fragments and protons taken from separate events. Analysis of these uncorrelated events proceeded in parallel with the real data, and it was found at each stage that the observed trends were not due to detector biases.

III. RESULTS

The average transverse momenta in the reaction plane resulting from Gaussian fits to the P^x distributions are shown in Fig. 3 for protons produced in C+C and C+Au reactions. The general trends of the data share two important characteristics with

results obtained for peripheral events in 45 MeV/nucleon Ar+Al reactions by Sullivan et al.⁷ and 200 MeV/nucleon Au+Fe reactions by Harris et al.¹³ The data from all four systems show an offset in the negative P^x direction (away from the projectile fragment), and a positive slope at mid-rapidity. We will investigate the cause of the offset first.

The authors of Ref. 13 suggested that the offset was a signature of attractive deflection of light particles by the nuclear mean field, but the authors of Ref. 7 connected the effect with momentum conservation, arguing that the negative $\langle P^x \rangle$ of the light particles was balanced by the positive $\langle P^x \rangle$ of the projectile fragments. The latter explanation is in agreement with the results of light particle - projectile fragment coincidence experiments (Ref. 14 and references therein) in which the authors found that particles produced in the hot mid-rapidity region were best characterized by a source whose velocity had a recoil component directed away from the projectile fragment. The recoil scenario is most strongly supported by the data of Rabe et al.¹⁵ for 84 MeV/nucleon O induced reactions on Ni and Au targets. They found enhanced light particle emission on the opposite side of the beam from the projectile fragment, and the enhancement increased linearly with projectile fragment transverse momentum. In our C+C data, the linear relationship between the proton P_x^0 offset and the transverse momentum of the projectile fragment, shown in Fig. 4, demonstrates that the offset is a recoil due to momentum conservation.

Most of the light particle - projectile fragment coincidence studies that were interpreted in terms of a recoiling mid-rapidity source were performed using asymmetric systems.¹⁴ Thus it may be considered surprising that the effect is present in the symmetric C+C system since it would be expected that the transverse momentum of

the projectile fragment would be balanced by the momentum of the target fragment, leaving the mid-rapidity source on the average with no net transverse momentum. This apparent contradiction can be resolved by noting that the mid-rapidity region contains nucleons donated by the projectile, and the partition of momentum between the projectile fragment and its contribution to the mid-rapidity source will introduce a relative momentum between the two for each event. When the projectile fragment is deflected in its interaction with the target, a transverse momentum separation in the reaction plane is created between the projectile fragment and the mid-rapidity source. Events in which the momentum partition between the projectile fragment and the nucleons donated by the projectile to the mid-rapidity source acts to increase this transverse momentum separation result in a mid-rapidity source recoil away from the projectile fragment, larger projectile fragment deflection angles, and hence an enhanced probability of detection. Thus the negative offset is not in itself a signature of attractive deflection of light particles, but of momentum conservation.

In contrast to the results of Rabe et al.¹⁵ who found a nearly identical recoil for reactions with the heavy Au target and the lighter Ni target, we show in Fig. 4 that the recoil effect is strongly suppressed for the Au target. This implies that nearly the entire gold nucleus participated in the recoil, making the P_0^* per proton insensitive to the P^* of the projectile fragment. This result is consistent with conclusions drawn from the analysis of peripheral 35 MeV/nucleon O+Ni collisions¹⁶ which supported strong target participation in the emission of intermediate velocity alphas. For the 50 MeV/nucleon C induced reactions, the mid-rapidity protons may be originating from a hot spot on the Au target, while the 84 MeV/nucleon O induced reactions may form a detached mid-rapidity source.

The second feature common to the transverse momenta versus rapidity data presented in Ref. 7, Ref. 13, and the present work is their positive slope at mid-rapidity. In our C+C and C+Au data, the slope at mid-rapidity is determined by the presence of a peak in P_x^a near the projectile fragment rapidity. Therefore, it is necessary to investigate the influence of projectile fragment sequential decay.

Two pieces of evidence show that the peak at the fragment rapidity is due to sequential decay. First, when we examine the proton P_x^a distribution at the fragment rapidity we find two distinct components, one of which can be associated with projectile fragment decay. A fit to the high $|P_x^a|$ tails of the distribution produces a broad Gaussian centered on the negative side of the beam axis, while an improved fit is obtained by including a narrower Gaussian offset towards the positive side. This is demonstrated in Fig. 5 in which we display the P_x^a distribution of protons detected with a velocity parallel to the beam axis equal to that of the average projectile fragment. The low momentum region which is affected by our energy thresholds is not plotted. In the upper panel of the figure, we have restricted a Gaussian fit to the high $|P_x^a|$ tails of the momentum distribution, $|P_x^a| \geq 250 \text{ MeV}/c$. The lack of agreement between the data and the fit at low $|P_x^a|$ values indicates the presence of an additional source of protons offset toward the projectile fragment side of the reaction plane at low $|P_x^a|$.

In the lower panel of Fig. 5 we have attempted to study both sources using a simultaneous double Gaussian fit. Although the two distributions, indicated by dashed lines, are not well separated, the general features are of a broad (hot) distribution with a negative P_x^a and a narrower (cooler) distribution with a positive P_x^a . Using the relationship $\sigma = \sqrt{m\tau}$, where σ is the width of the Gaussian and m is the mass of a

proton, temperatures τ of ≈ 10 MeV and ≈ 5 MeV are obtained for the two sources. The peak in the P_x^* at the average projectile fragment rapidity is thus produced by a cool momentum distribution on the same side of the beam as the fragments. We conclude that, even though protons in the Forward Array were excluded from the analysis, we are still getting a contribution from projectile fragment sequential decay.

This interpretation can be tested by examining the shape of relative momentum distributions. The circles in the upper portion of Fig. 6 represent the ΔP distribution between protons detected in the Main Ball and coincident projectile fragments in the Forward Array. We have divided the observed ΔP of each pair by the ΔP that would be expected due to Coulomb repulsion. The distributions in the upper panels were then divided by random distributions created by pairing protons with projectile fragments from different events to create the correlation functions shown in the lower panels. A strong correlation is observed for $\Delta P \approx \Delta P_{Coulomb}$, indicating the presence of projectile fragment sequential decay products in our proton sample. Thus we conclude that the positive slope of the data at mid-rapidity in Fig. 3 is primarily due to the combination of an overall negative offset due to momentum conservation and a positive offset at $y = y_{frag}$ due to sequential decay, rather than mean field deflection.

In order to study the hot mid-rapidity source of protons, we then excluded protons with a $|P_x^*| \leq 250 \text{ MeV}/c$ from the Gaussian fits. This minimizes the effect of protons produced by cool sequential decay of the projectile fragment and is the largest practical cut that still allows us to characterize the P_x^* distributions. The resulting data are denoted by crosses in Fig 6. They demonstrate that the kinematical region dominated by projectile fragment sequential decay has been eliminated. For C+C, a correlation remains at high ΔP values, corresponding to the recoil effect discussed

previously.

Using this high $|P^x|$ gate, we display in Fig. 7 P_0^x vs. rapidity for the hot participant source. Isolating this source has removed the peak at the projectile fragment velocity, revealing a *negative* slope at mid-rapidity. Three points on either side of $y = \frac{1}{2}y_{beam}$ were fit with a straight line. For C+C we find the slope ($\frac{dP_0^x}{dy}$) to be -26 ± 3 MeV/c, while for C+Au we obtain -33 ± 6 MeV/c. This mid-rapidity slope, when multiplied by the beam rapidity in the center of mass system, is the "flow" parameter extracted from heavy-ion collisions at higher beam energies.¹² The point at which the line crosses the rapidity axis corresponds to a velocity of -0.47 ± 0.02 c for the C+C system due to the negative offset discussed earlier. The C+Au system show a crossing point of 0.06 ± 0.05 c, consistent with the velocity of the center of mass. There is a increase in P_0^x at high rapidities that may be due to contamination from the tail of the sequential decay distribution. At high rapidities, the cross section for participant protons decreases relative to that for sequential decay, so we would expect that the simple $|P^x|$ gate would no longer be sufficient to isolate the participant source.

IV. DISCUSSION

Since the angular acceptances extend down to the grazing angle for the C+Au system, approximately 6° , and since the fragments are only lightly damped, we can assume that the fragments in the peak were positively deflected by the repulsive Coulomb interaction. Although the grazing angle for the C+C reaction is less than 1° , a similar lightly damped peak is present. If we take the projectile fragments as being positively scattered, then the negative slope in the P_0^x distribution implies that the participant protons were simultaneously attractively deflected.

We do not expect that the projectile fragments that we detected were negatively deflected because they were weakly damped. As a check, we repeated the analysis dividing the events into projectile fragment velocity bins of weaker damping ($v_{frag.} \geq 85\% v_{beam}$) and stronger damping ($\approx 70\% v_{beam} \leq v_{frag.} \leq 80\% v_{beam}$). The overall trends of both data sets were identical to the velocity summed data, indicating that the fragments and the participant protons are deflected in opposite directions down to fragment velocities of $\approx \frac{3}{4}v_{beam}$. For the above reasons, it is possible that the data⁷ on attractive flow as a function of impact parameter may be incorrect for the more peripheral reactions.

Projectile fragmentation models which pre-divide the projectile prior to its collision with the target show similar behavior^{14,17,18}; ie. lightly damped projectile fragments are Coulomb trajectory dominated, but the participant part of the projectile that undergoes friction is slowed and deflected attractively. Simple projectile fragmentation alone cannot account for our observations, however, because the C+Au data does not exhibit a strong recoil relationship between the projectile fragment and the participant proton source.

For reaction plane determination, this interplay between attractive and repulsive forces in peripheral events makes the application of the commonly used global transverse momentum analysis¹⁹ problematic when both projectile fragments and mid-rapidity light particles are detected. Since this technique assumes that the particles flow primarily in the same direction, restricting consideration to only the projectile fragments and their sequential decay products should allow for unambiguous characterization of the reaction plane. Light particles in the mid-rapidity region should only be included with a weight that reflects their different flow direction.

This new approach to the analysis of peripheral heavy-ion collisions is promising since it provides both the magnitude and the *direction* of the transverse momentum flow. Use of lightly damped projectile fragments to find the reaction plane should allow experimenters to observe directly the change in the sign of the flow as the beam energy is increased from the regime in which the attractive interaction dominates to that where repulsive nucleon-nucleon scattering takes over.

ACKNOWLEDGMENTS

The authors would like to thank Professor Pawel Danielewicz and Professor Gordon Wozniak for their helpful comments. This work was supported in part by the National Science Foundation under Grant No. PHY-89-13816.

*Present address: Lawrence Berkeley Laboratory, Berkeley CA 94720, USA.

†Present address: Lawrence Livermore National Laboratory, Livermore CA 94550, USA.

‡Present address: Department of Physics, University of Michigan, Dearborn MI 48128, USA.

§Present address: Gesellschaft für Schwerionenforschung, D-6100 Darmstadt, Fed. Rep. Germany.

¹G.F. Bertsch, W.G. Lynch, and M.B. Tsang, *Phys. Lett.* **189B**, 384 (1987)

²C.A. Ogilvie, W. Bauer, D.A. Cebra, S. Howden, J. Karn, A. Nadasen, A. Vander Molen, G.D. Westfall, W.K. Wilson, and J.S. Winfield, *Phys. Rev. C* **42**, R10

(1990)

- ³D. Krofcheck, D.A. Cebra, M. Cronqvist, R. Lacey, T. Li, C.A. Ogilvie, A. Vander Molen, K. Tyson, G.D. Westfall, W.K. Wilson, J.S. Winfield, A. Nadasen, and E. Norbeck, *Phys. Rev. C*, in press
- ⁴D. Krofcheck, W. Bauer, G.M. Crawley, C. Djalali, S. Howden, C.A. Ogilvie, A. Vander Molen, G.D. Westfall, W.K. Wilson, R.S. Tickle, and C. Gale, *Phys. Rev. Lett.* **63**, 2028 (1989)
- ⁵D. Krofcheck, W. Bauer, G.M. Crawley, S. Howden, C.A. Ogilvie, A. Vander Molen, G.D. Westfall, W.K. Wilson, R.S. Tickle, C. Djalali, and C. Gale, submitted to *Phys. Rev. C*
- ⁶W.M. Zhang, R. Madey, M. Elaasar, J. Schambach, D. Keane, B.D. Anderson, A.R. Baldwin, J. Cogar, J.W. Watson, G.D. Westfall, G. Krebs, and H. Wieman, *Phys. Rev. C* **42**, R491 (1990)
- ⁷J.P. Sullivan, J Péter, D. Cussol, G. Bizard, R. Brou, M. Louvel, J.P. Patry, R. Regimbart, J.C. Steckmeyer, B. Tamain, E. Crema, H. Doubre, K. Hagel, G.M. Jin, A. Péghaire, F. Saint-Laurent, Y. Cassagnou, R. Lebrun, E. Rosato, R. Macgrath, S.C. Jeong, S.M. Lee, Y. Nagashima, T. Nakagawa, M. Ogihara, J. Kasagi, and T. Motobayashi, *Phys. Lett.* **249B**, 8 (1990)
- ⁸M.B. Tsang, G.F. Bertsch, W.G. Lynch, and Mitsuru Tohyama, *Phys. Rev. C* **40**, 1685 (1989)
- ⁹M.B. Tsang, R.M. Ronningen, G. Bertsch, Z. Chen, C.B. Chitwood, D.J. Fields, C.K. Gelbke, W.G. Lynch, T. Nayak, J. Pochodzalla, T. Shea, W. Trautmann,

Phys. Rev. Lett. **57**, 559 (1986)

- ¹⁰K Asahi, M. Ishihara, H. Takanashi, M. Koguchi, M. Adachi, M. Fukuda, N. Inabe, D. Mikolas, D. Morrissey, D. Beaumel, T. Ichihara, T. Kubo, T. Shimoda, H. Miyatake, and N. Takahashi, RIKEN preprint, RIKEN-AF-NP-87
- ¹¹G.D. Westfall, J.E. Yurkon, J. Van der Plicht, Z.M. Koenig, B.V. Jacak, R. Fox, G.M. Crawley, M.R. Maier, and B.E. Hasselquist, Nucl. Instr. and Meth. **A238**, 347 (1985)
- ¹²H.H. Gutbrod, A.M. Poskanzer, and H.G. Ritter, Rep. Prog. Phys. **52**, 1267 (1989)
- ¹³J.W. Harris, B.V. Jacak, K.-H. Kampert, G. Claesson, K.G.R. Doss, R. Ferguson, A.I. Gavron, H.-A. Gustafsson, H. Gutbrod, B. Kolb, F. Lefebvres, A.M. Poskanzer, H.-G. Ritter, H.R. Schmidt, L. Teitelbaum, M. Tincknell, S. Weiss, H. Wieman, and J. Wilhelmy, Nucl. Phys. **A471**, 241c (1987)
- ¹⁴R. Wada, D. Fabris, M. Gonin, M. Gui, K. Hagel, Y. Lou, D. Utley, J.B. Natowitz, G. Nebbia, R. Billerey, B. Cheynis, A. Demeyer, D. Drain, D. Guinet, C. Pastor, L. Vagneron, K. Zaid, J. Alarja, A. Giorni, D. Heuer, C. Morand, B. Viano, C. Mazur, C. Ngô, S. Leray, R. Lucas, M. Ribrag, and E. Tomasi, Texas A&M Cyclotron Institute preprint, #90-10, submitted to Phys. Rev. C
- ¹⁵H.J. Rabe, K.D. Hildenbrand, U. Lynen, W.F.J. Müller, H. Sann, H. Stelzer, W. Trautmann, R. Trockel, R. Wada, J. Pochodzalla, E. Eckert, P. Kreutz, A. Kühmichel, N. Brummund, R. Glasow, K.H. Kampert, R. Santo, and D. Pelte, Phys. Lett. **196B**, 439 (1987)
- ¹⁶P.L. Gonthier, J.D. Lenters, M.T. Vonk, D.A. Cebra, W.K. Wilson, A. Vander

Molen, J. Karn, S. Howden, A. Nadasen, J.S. Winfield, and G.D. Westfall, submitted to Phys. Rev. C

¹⁷K. Möhring, T. Srokowski, D.H.E. Gross, and H. Homeyer, Phys. Lett. **203B**, 210 (1988)

¹⁸G. Royer, Y. Raffray, A. Oubahadou, and B. Remaud, Nucl. Phys. **A466**, 139 (1987)

¹⁹P. Danielewicz and G. Odyniec, Phys. Lett. **157B**, 146 (1985)

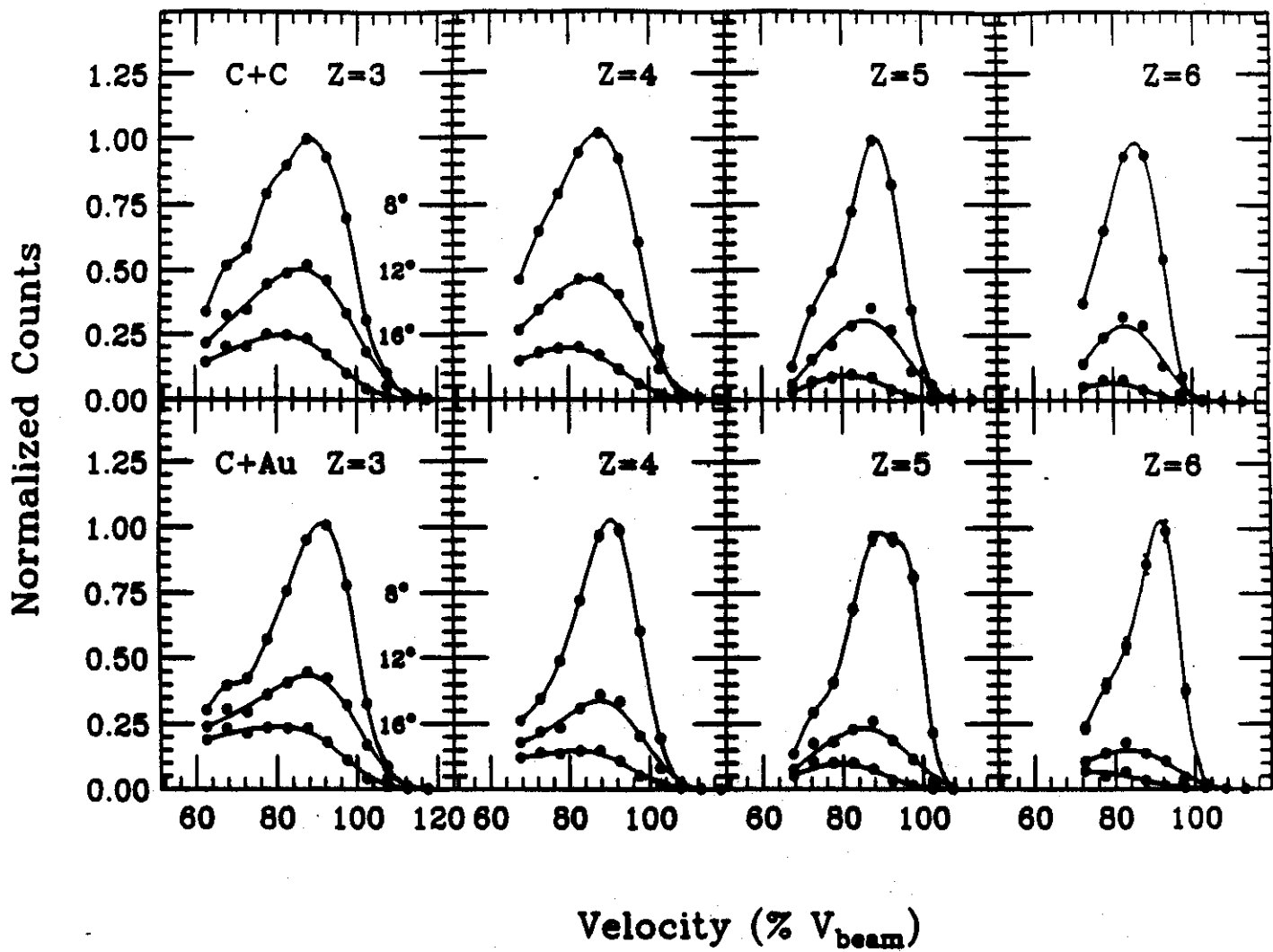


FIG. 1. Velocity spectra for projectile fragments detected in the Forward Array in coincidence with protons in the Main Ball for 50 MeV/nucleon C+C (upper panels) and C+Au (lower panels).

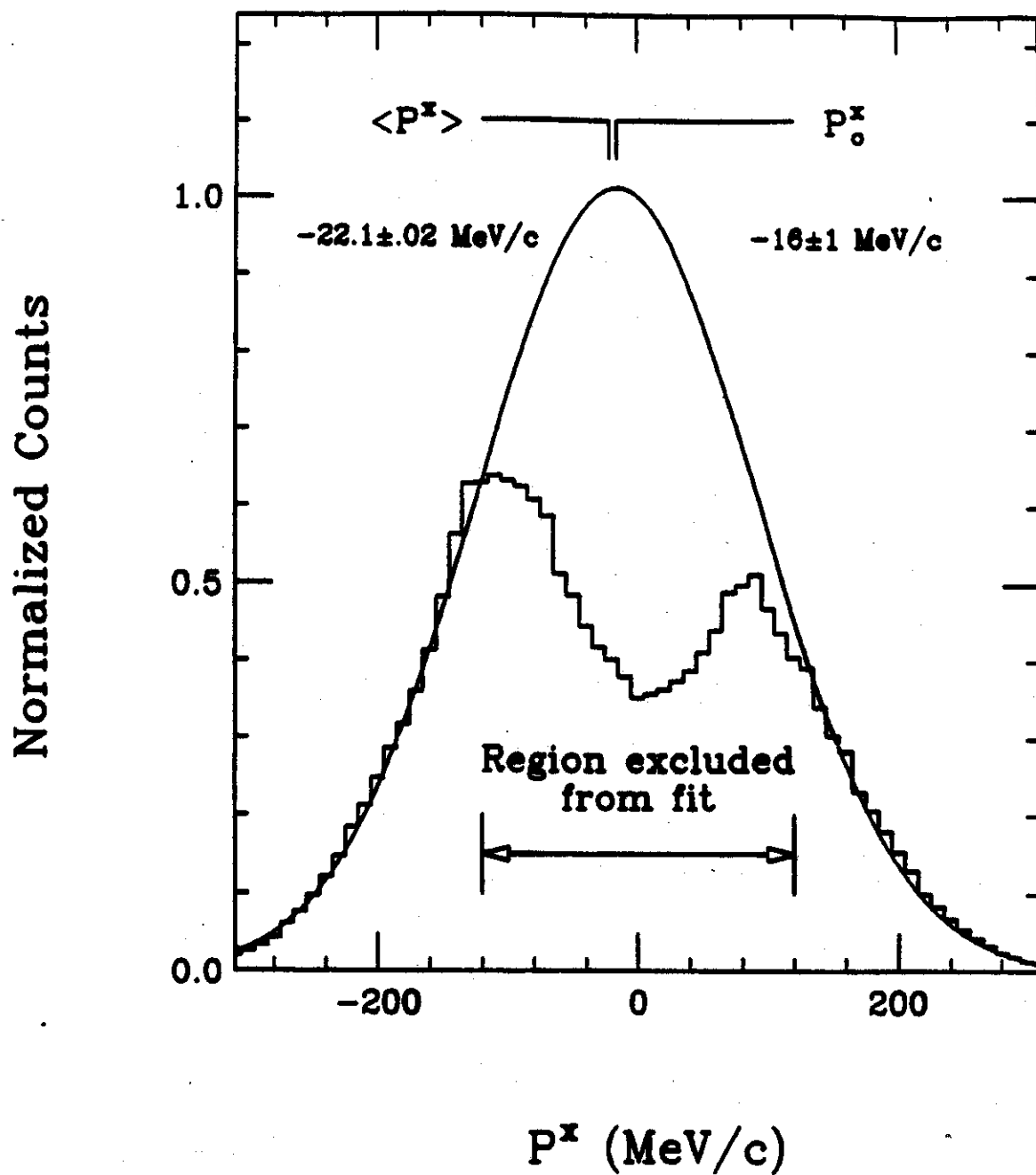


FIG. 2. Histogram of the transverse momentum distribution projected on to the reaction plane for mid-rapidity protons detected by the Main Ball in C+C reactions. The valley around $P^x \approx 0$ MeV/c is due to detector low energy thresholds and was excluded from the Gaussian fit which is shown as a solid curve.

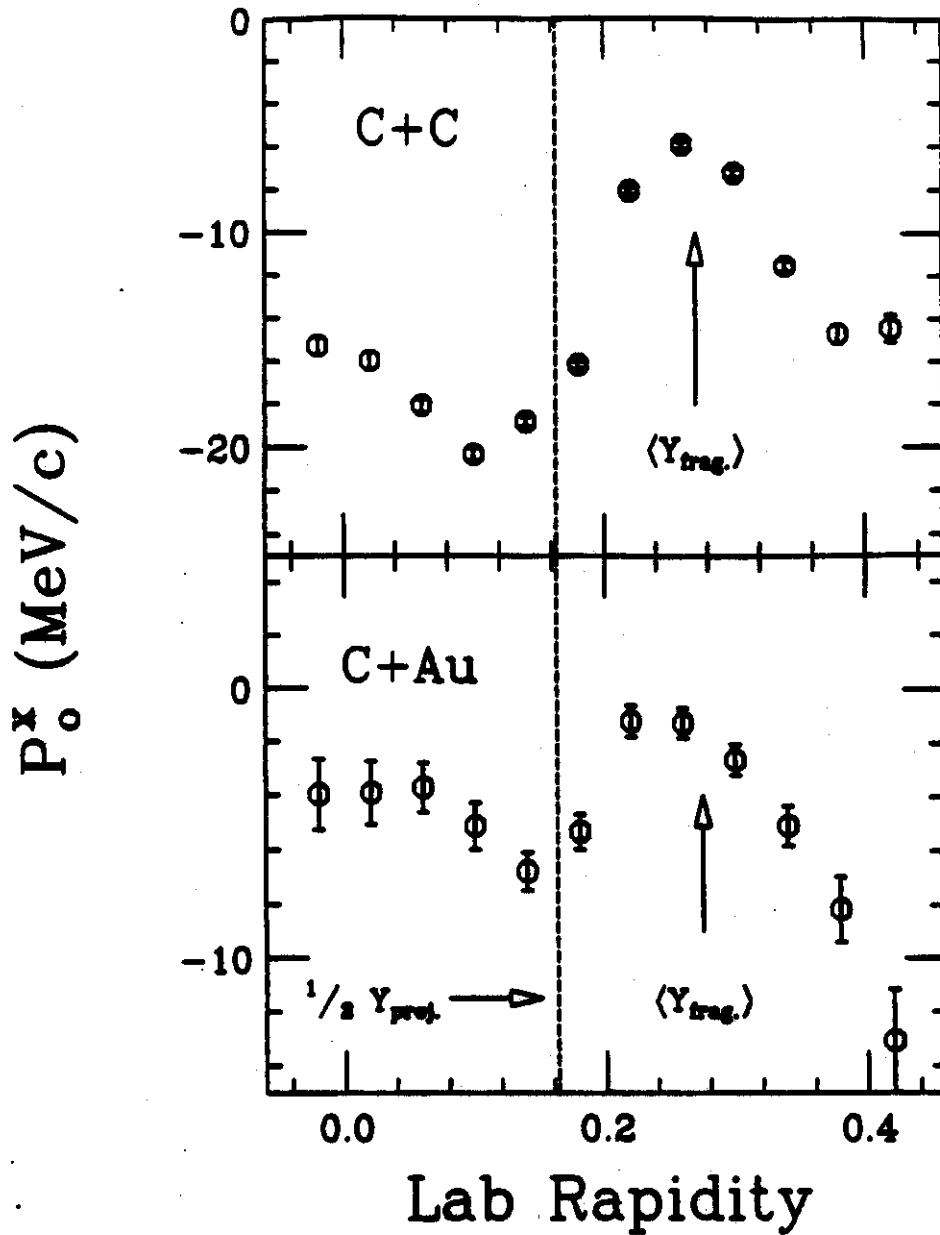


FIG. 3. The center of the transverse momentum distribution in the reaction plane as a function of rapidity for C+C (upper panel) and C+Au (lower panel). The centers were extracted using single Gaussian source fits as described in the previous figure and the error bars reflect the uncertainties of the fits.

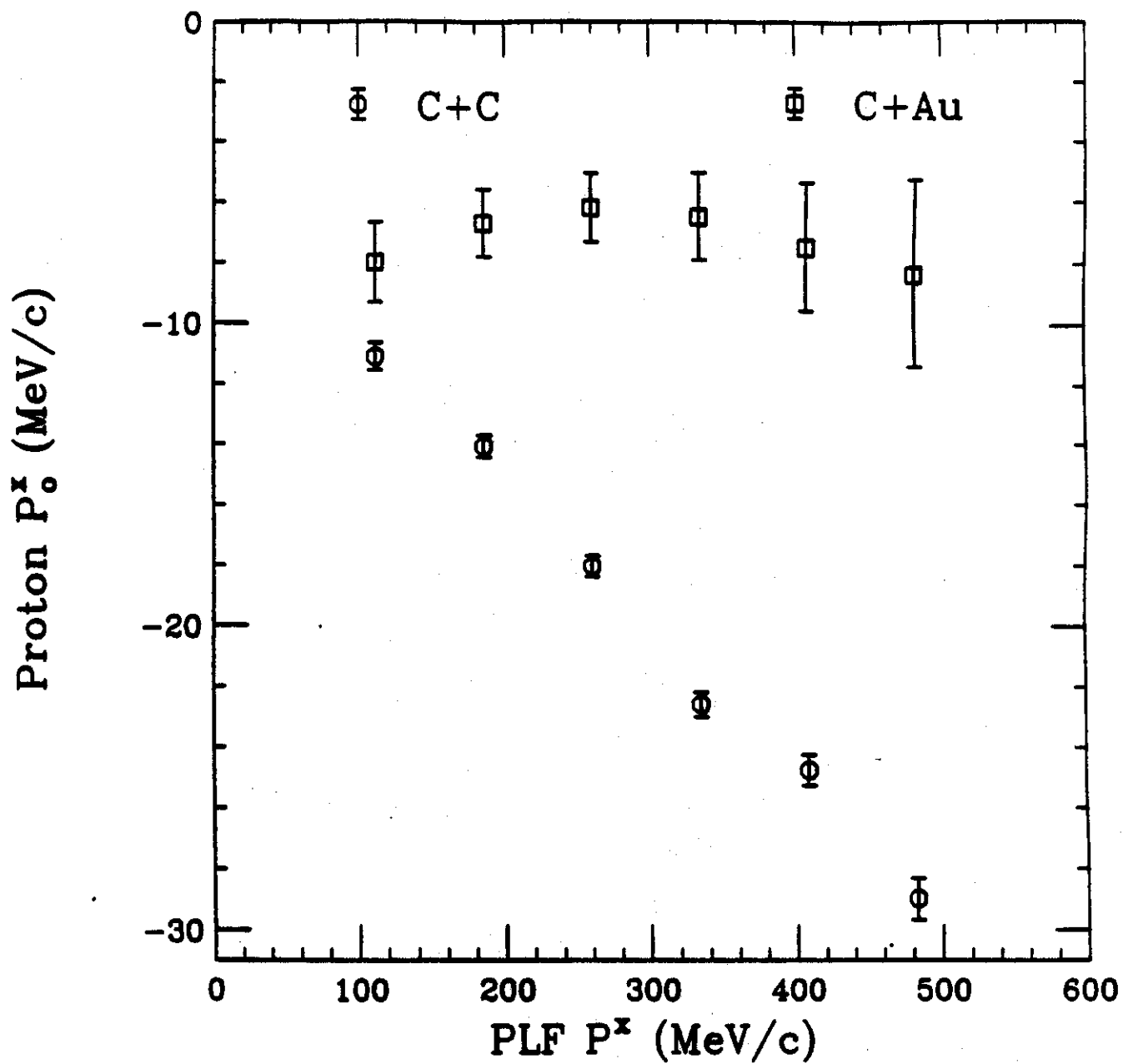


FIG. 4. The negative offset for the center of the mid-rapidity proton source is shown as a function of the transverse momentum of the projectile fragment for C+C (circles) and C+Au (squares) collisions.

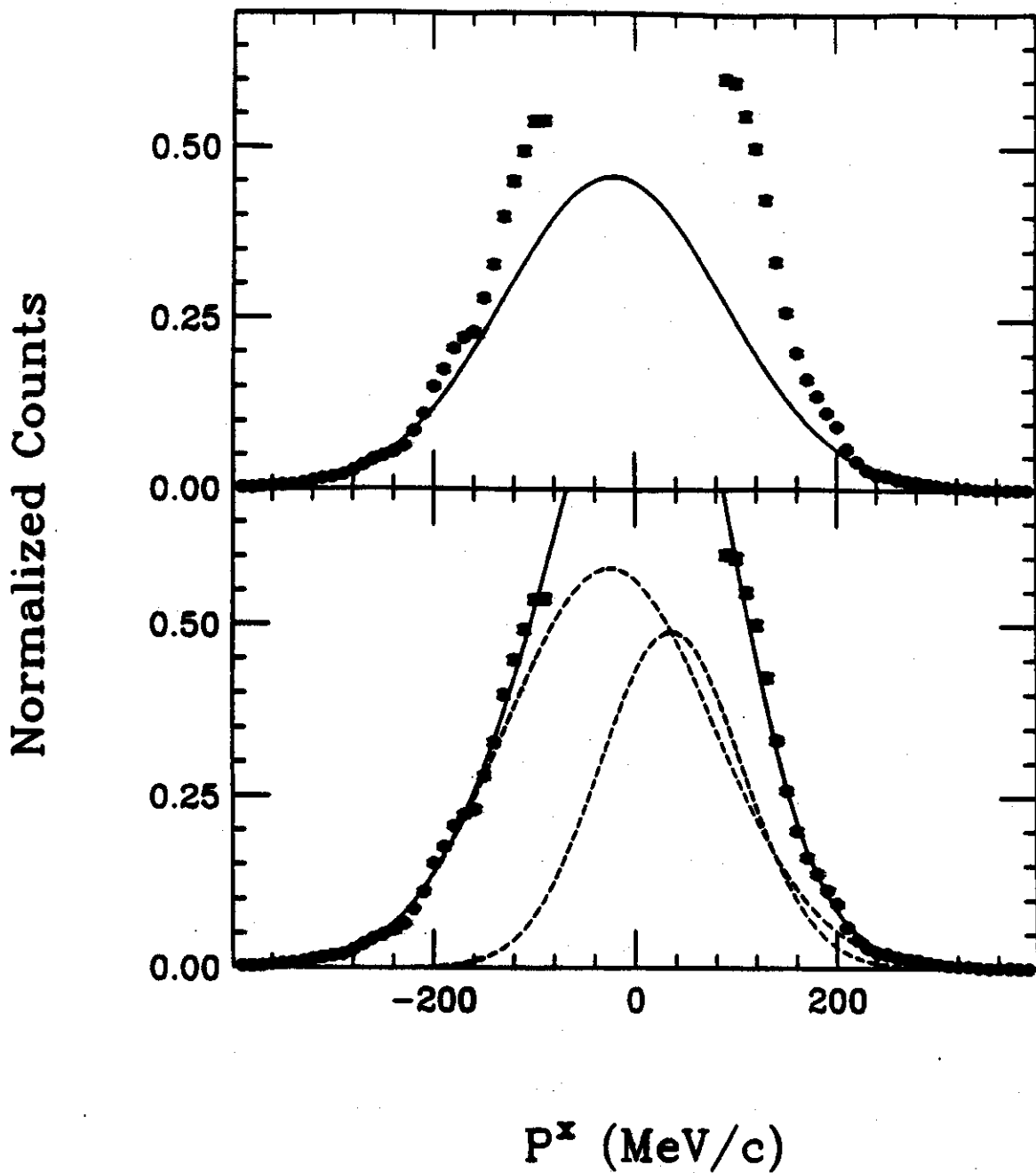


FIG. 5. The proton transverse momentum distribution projected on the reaction plane for C+C reactions, gated on proton rapidities near the average rapidity of the projectile fragment. In the top panel, the high $|P^x|$ tails of the distribution have been fit using a single Gaussian source (solid curve), which is unable to account for the low $|P^x|$ region. In the lower panel two Gaussian sources (dashed curves) are able to fit simultaneously the entire P^x distribution.

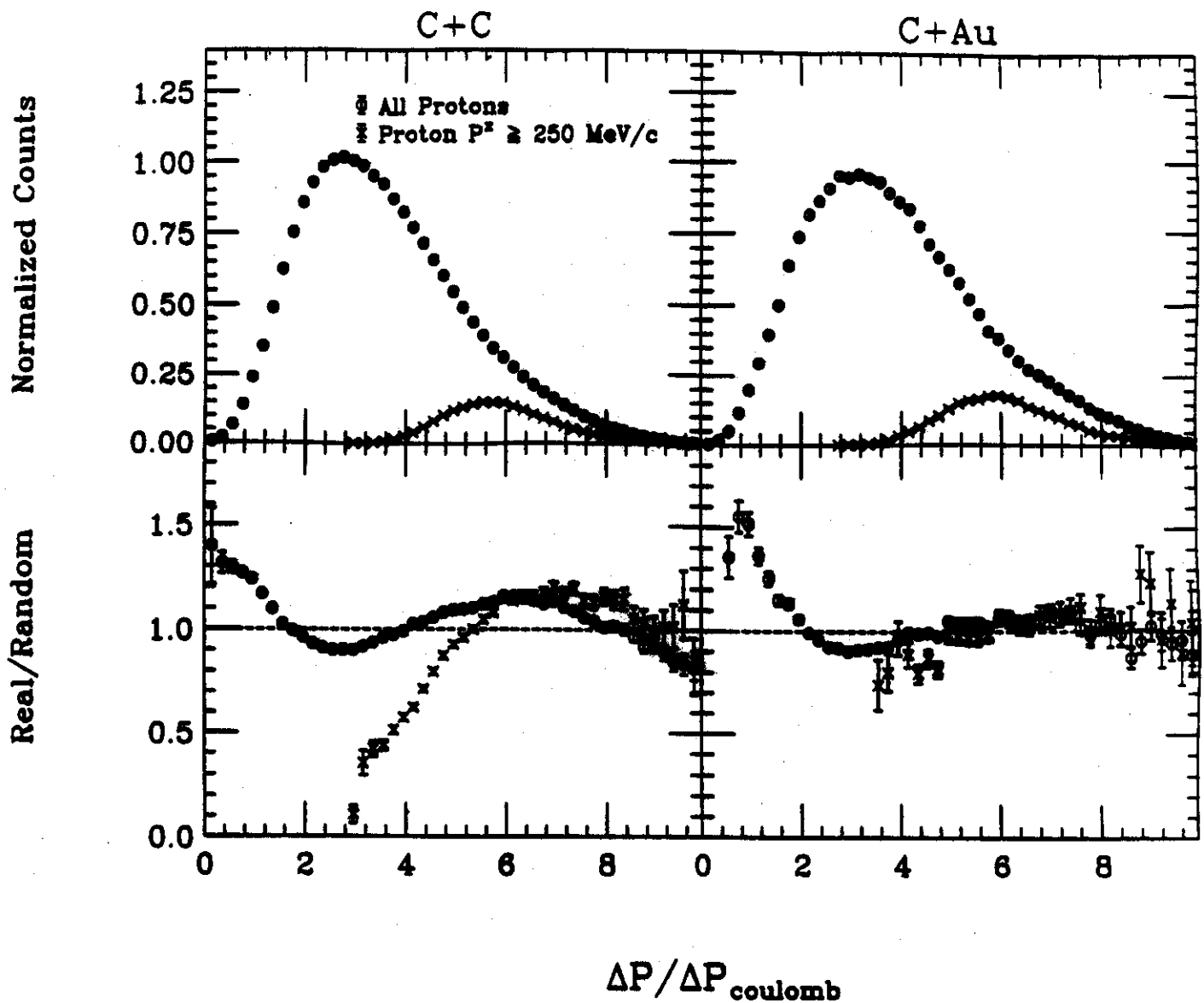


FIG. 6. Yields (upper panels) and correlation functions (lower panels) for C+C (left hand panels) and C+Au (right hand panels) reactions. The momentum difference, ΔP , has been divided by the expected momentum kick due to Coulomb repulsion. The data denoted by circles include all protons in coincidence with projectile fragments; the contribution from fragment sequential decay is minimized for the data denoted by crosses.

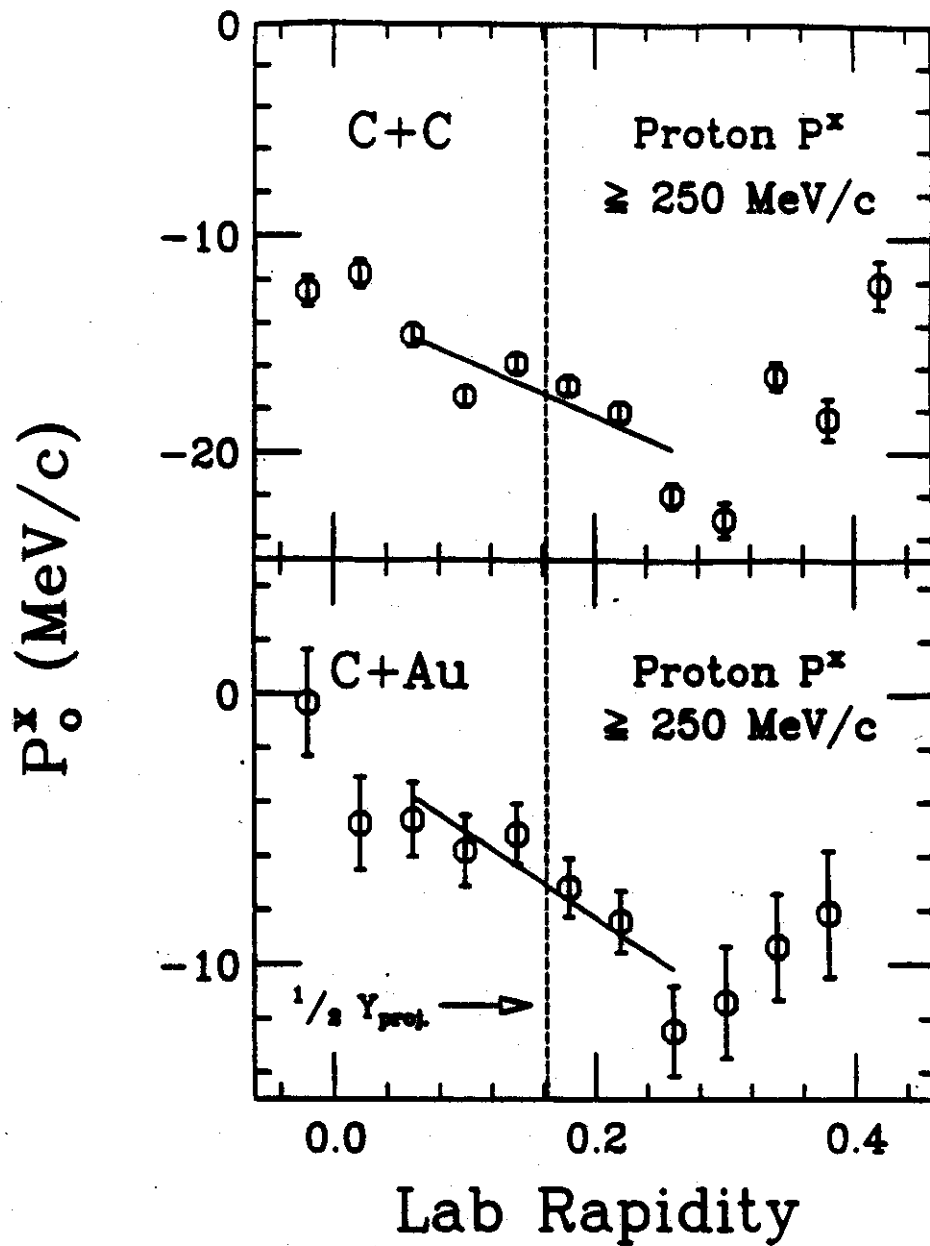


FIG. 7. The center of the transverse momentum distribution in the reaction plane as a function of rapidity for C+C (upper panel) and C+Au (lower panel). The centers were extracted using single Gaussian source fits to the participant protons ($|P^x| \geq 250$ MeV/c) and show a negative slope at mid-rapidity (solid line).